nanomaterials

MDPI

Article

Co-Doped $NdFeO_3$ Nanoparticles: Synthesis, Optical, and Magnetic Properties Study

Tien Anh Nguyen [1,2], Thanh Le Pham [3], Irina Yakovlevna Mittova [4], Valentina Olegovna Mittova [5], Truc Linh Thi Nguyen [3], Hung Van Nguyen [6] and Vuong Xuan Bui [7,*]

1 Informetrics Research Group, Ton Duc Thang University, Ho Chi Minh City 700000, Vietnam; nguyenanhtien@tdtu.edu.vn
2 Faculty of Applied Sciences, Ton Duc Thang University, Ho Chi Minh City 700000, Vietnam
3 Faculty of Chemistry, Ho Chi Minh City University of Education, Ho Chi Minh City 700000, Vietnam; thanhhoahoc@gmail.com (T.L.P.); linhntt@hcmue.edu.vn (T.L.T.N.)
4 Faculty of Chemistry, Voronezh State University, Voronezh 394018, Russia; imittova@mail.ru
5 Department of Biochemistry, Voronezh State Medical University Named after N. N. Burdenko, Voronezh 394036, Russia; vmittova@mail.ru
6 Practice and Experimental Center for Dong Thap University, Cao Lanh City 81000, Vietnam; nguyenvanhung@dthu.edu.vn
7 Faculty of Pedagogy in Natural Sciences, Sai Gon University, Ho Chi Minh City 700000, Vietnam
* Correspondence: buixuanvuongsgu@gmail.com

Abstract: In this work, single-phase nanostructured $NdFe_{1-x}Co_xO_3$ (x = 0, 0.1, 0.2, and 0.3) perovskite materials were obtained by annealing stoichiochemistry mixtures of their component hydroxides at 750 °C for 60 min. The partial substitution of Fe by Co in the $NdFeO_3$ crystal lattice leads to significant changes in the structural characteristics, and as a consequence, also alters both the magnetic and optical properties of the resulting perovskites. The low optical band gap (E_g = 2.06 ÷ 1.46 eV) and high coercivity (H_c = 136.76 ÷ 416.06 Oe) give Co-doped $NdFeO_3$ nanoparticles a huge advantage for application in both photocatalysis and hard magnetic devices.

Keywords: nanocrystals; co-doped $NdFeO_3$; co-precipitation method; optical properties; magnetic properties

Citation: Nguyen, T.A.; Pham, T.L.; Mittova, I.Y.; Mittova, V.O.; Nguyen, T.L.T.; Nguyen, H.V.; Bui, V.X. Co-Doped $NdFeO_3$ Nanoparticles: Synthesis, Optical, and Magnetic Properties Study. *Nanomaterials* **2021**, *11*, 937. https://doi.org/10.3390/nano11040937

Academic Editor: Alexander Kromka

Received: 25 February 2021
Accepted: 2 April 2021
Published: 6 April 2021

1. Introduction

Perovskite orthoferrite materials have been intensively studied because of their diverse unique properties, variable formulae, variable structures, and wide technological applications. Especially, the substitution of Ln or Fe sites of the $LnFeO_3$ perovskite-type oxides (where Ln is a rare-earth element such as La, Nd, and Pr) by other elements which can exhibit considerable multi-valence and defect sites in their structures, which lead to the tunable redox and electromagnetic characteristics of the materials [1–3]. In order to boost the performances and widen the applications of perovskite materials, much effort has been spent to downscale the structure into nano size. Indeed, in comparison with their bulk counterparts, perovskite nanomaterials show many advantages, such as high processing capability of thin film [4], rich and controllable catalyst active sites [5,6] or excellent optical, electrical, and magnetic properties [7–9].

In $NdFeO_3$, the magnetic moments of Fe and Nd are two antiparallel coupled nonequivalent magnetic sublattices. The electrons in the 3d and 4f orbitals of these two sublattices interact with spin-lattice coupling, leading to a very unstable magnetic state and, thus, they result in unusually large magnetic anisotropy, magnetization reversal, and spin switching in low magnetic fields [10]. In order to adjust their optical, electrical, and magnetic properties and to enhance the performance of pristine perovskite, transition metal ions can be doped into their crystal lattices. Co-doped $LnFeO_3$ materials have attracted extensive study thanks to their exciting dielectric, sensing, optical, and magnetic properties. Owing

to the multiple spins and oxidation states of Co, the process of catalysts may be modified by changing the concentration of Co in solid solutions [3,6,11–14].

Several studies [15–20] described the formation of $LnFeO_3$ orthoferrites nanoparticles (Ln = La, Y), including those doped with metals (for example, Mn, Co, Ni, and Ba) by a simple co-precipitation method via the hydrolysis of cations in boiling water followed by the addition of appropriate precipitants. In our recent work [21], $NdFeO_3$ nanoparticles, of 30 nm in size, were obtained via the simple co-precipitation method mentioned above, their crystal structure and magnetic properties were also studied therein.

In this paper, single-phase Co-doped $NdFeO_3$ nanoparticles were synthesized and the changes in their crystal structure, their magnetic and optical properties were also studied. To the best of our knowledge, similar work has not been reported elsewhere.

2. Materials and Methods

All reagents in this work are analytical grade and were used without any further purification. The procedure for synthesizing Co-doped $NdFeO_3$ nanoparticles is similar to that of $NdFeO_3$ [21], with NaOH 5% as the precipitant instead of a NH_3 5% solution, in order to avoid the generation of soluble complex from the reaction of cobalt (II) hydroxide precipitate ($Co(OH)_2\downarrow$) and ammonium solution according to Equation (1) [22].

$$Co(OH)_2\downarrow + 6NH_3 \rightarrow [Co(NH_3)_6](OH)_2 \quad (1)$$

The structure and phase composition of the samples were investigated by X-ray powder diffraction (XRD, D8-ADVANCE, Brucker, Bremen, Germany) with Cu K_α radiation (λ = 1.54056 Å), the step size is chosen to be 0.02 in range of 10° to 80°. The average crystal size was determined according to the Debye–Scherrer equation [23]; lattice constants *a*, *b*, *c*, and the unit cell volume *V* were determined using the Rietveld method [23] implemented in the X'pert High Score Plus 2.2b software package [18–20].

The energy-dispersive X-ray spectroscopy (EDX) was carried out with a FE-SEM S-4800 spectrometer (Hitachi, Tokyo, Japan). The average value of five different positions in each sample was taken as the final result of the corresponding sample. Particle size and morphology of Co-doped $NdFeO_3$ nanoparticles were determined using transmission electron microscopy (TEM; JEOL-1400, Jeol Ltd., Tokyo, Japan).

The UV-Vis absorption spectra of $NdFe_{1-x}Co_xO_3$ nanocrystals were studied on a UV-Visible spectrophotometer (UV-Vis, JASCO V-550, Shimadzu, Tokyo, Japan). The optical energy gap (E_g, eV) was determined by fitting the absorption data to the direct transition as in previous publication [24].

Magnetic properties of the samples (the saturation magnetization M_s in the maximal field, the coercive force H_c and remanent magnetization M_r) were investigated at 300 K via a vibrating sample magnetometer (VSM, MICROSENE EV11, Tokyo, Japan).

3. Result and Discussion

3.1. Structures and Morphologies of Nanostructured $NdFe_{1-x}Co_xO_3$

The XRD patterns of the $NdFe_{1-x}Co_xO_3$ products (x = 0, 0.1, 0.2, 0.3, and 0.4) compared with those of the Nd_2O_3, Fe_2O_3, and Co_3O_4 component oxides independently prepared under similar conditions (annealed at 750 °C during 60 min) are shown in Figure 1. The annealing condition was determined according to the previous work [21]. Those patterns confirmed that the $NdFe_{1-x}Co_xO_3$ samples with x = 0, 0.1, 0.2, and 0.3 were pure orthoferrite phase perovskite structure ($NdFeO_3$, JCPDS No. 01-074-1473), with no identified peaks of oxide impurities. Interestingly, Co_3O_4 oxide was obtained instead of CoO since $Co(OH)_2$ hydroxide can be oxidized and decomposed after annealing at high temperature [24].

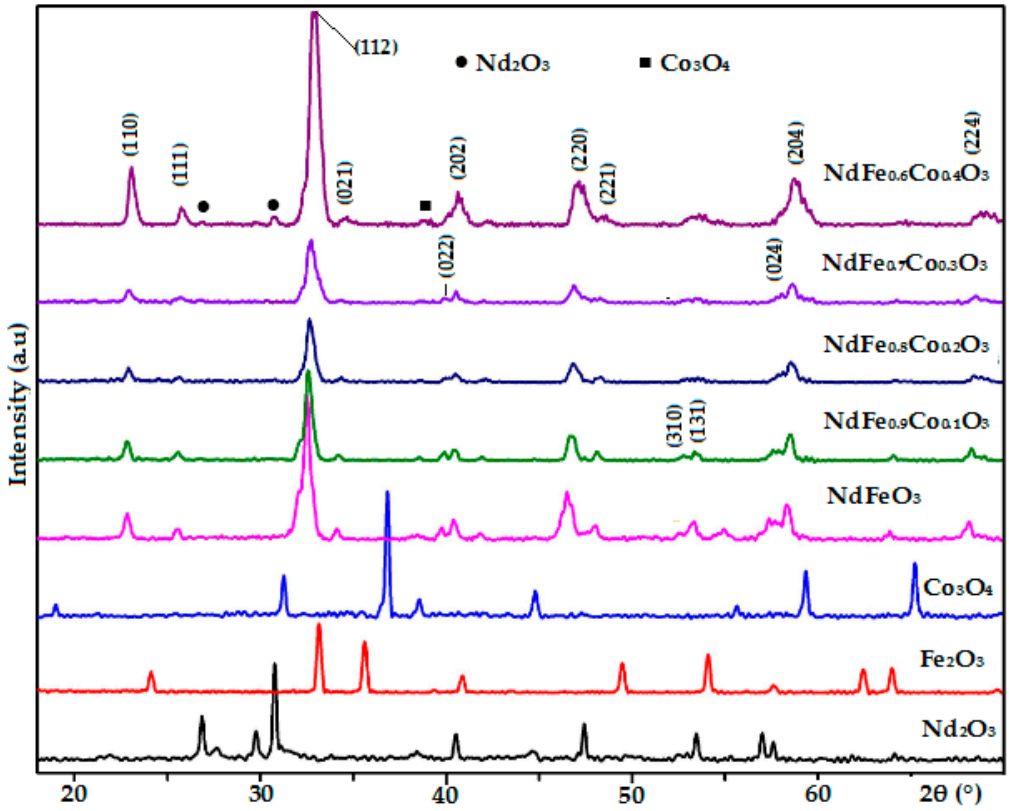

Figure 1. X-ray powder diffraction (XRD) patterns of $NdFe_{1-x}Co_xO_3$ samples (x = 0, 0.1, 0.2, 0.3, and 0.4) and Nd_2O_3, Fe_2O_3, and Co_3O_4 annealed at 750 °C for 60 min.

In the case of x = 0.4, aside from the peaks corresponding to the $NdFeO_3$ phase, there were peaks of the Nd_2O_3 phase (JCPDS No. 00-041-1089) at 2θ = 25.71 and 30.74°, and Co_3O_4 phase (JCPDS No. 00-043-1003) at 2θ = 38.87°. Thus, the successful substitution of Co into $NdFeO_3$ crystal structures only took place when x was less than 0.4. With the increase in Co concentration, the XRD peak shifted toward a higher 2θ (right shift) and gradually broadened while the intensity of peaks decreased. Consequently, there was a decrease in unit cell volume (from V = 238.56 to V = 233.29 Å^3) and in crystal size (from D_{XRD} = 28 ± 5 to D_{XRD} = 19 ± 3 nm) Figure 2 and Table 1. Such a decrease is also a confirmation for the Co (III) substitution to Fe (III) in the $NdFeO_3$ crystal lattice. The substitution of Fe^{3+} ions (r_{Fe3+} = 0.65 Å [24]) by smaller Co^{3+} ions (r_{Co3+} = 0.55 Å [24]) led to the reduction of the unit cell parameters and crystal size following Vegard's law, in which lattice parameters linearly varies with the degree of substitution of atoms or ions by others in ideal solid solution. The similar results were published in the previous research [12,13,18].

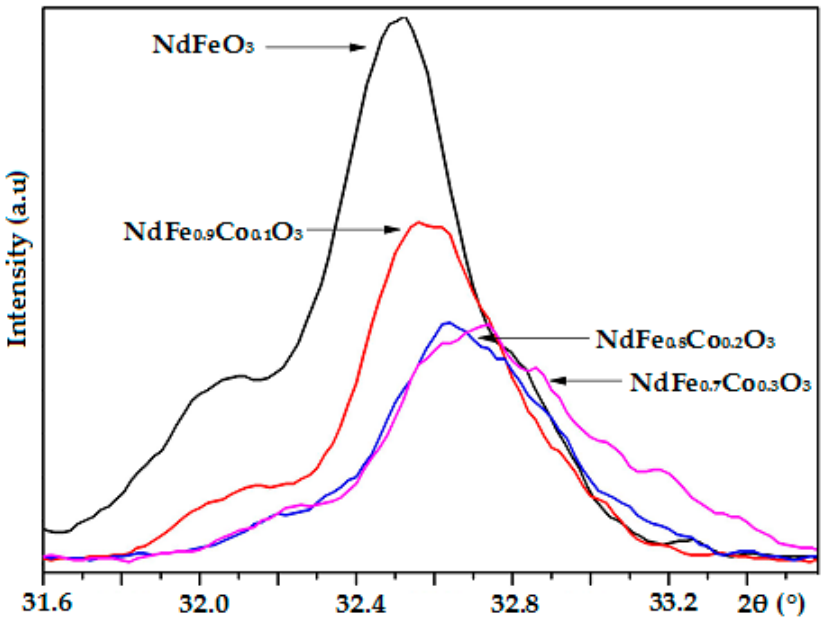

Figure 2. Slow-scan XRD patterns of peak (112) of $NdFe_{1-x}Co_xO_3$ samples annealed at 750 °C for 60 min.

Table 1. Lattice parameters and crystallite sizes of $NdFe_{1-x}Co_xO_3$ samples annealed at 750 °C for 60 min.

$NdFe_{1-x}Co_xO_3$	2θ° (112)	D_{avg}, nm		Lattice Constants, Å			*V*, Å^3
		XRD	TEM	*a*	*b*	*c*	
$NdFeO_3$ [21]	32.49	28 ± 5	-	5.4990	5.5910	7.7592	238.56
$NdFe_{0.9}Co_{0.1}O_3$	32.54	25 ± 3	47 ± 5	5.4257	5.5919	7.7638	235.55
$NdFe_{0.8}Co_{0.2}O_3$	32.57	22 ± 2	45 ± 6	5.4425	5.5292	7.7616	233.57
$NdFe_{0.7}Co_{0.3}O_3$	32.61	19 ± 3	42 ± 3	5.4113	5.5504	7.7673	233.29

TEM images and particle size distribution for $NdFe_{1-x}Co_xO_3$ samples (x = 0.1, 0.2, 0.3) are shown in Figure 3. As can be seen, the shape of the particles of the synthesized $NdFe_{1-x}Co_xO_3$ samples is close to spherical, but agglomerates of particles are noticeable. For the $NdFe_{0.9}Co_{0.1}O_3$ sample with the lowest level of cobalt doping, the particle size was in the range of 10–80 nm. The average particle diameter was 47 ± 5. For the other two samples ($NdFe_{0.8}Co_{0.2}O_3$ and $NdFe_{0.7}Co_{0.3}O_3$), the size of most particles was in the range of 20–70 nm. An analysis of the results of the size distribution of $NdFe_{1-x}Co_xO_3$ particles Figure 3 allows us to conclude that the average crystallite size decreases monotonically with an increase in the dopant content in the synthesized samples. The lower values of D_{avg} calculated based on the XRD data as compared to the TEM results were due to the peculiarities of the used methods. The determination of the average crystallite size by the calculation method according to the Debye–Scherrer formula leads to significant errors that can be caused by the choice of a mathematical model for analyzing the X-ray line profile for the determination of the particle size and the influence of various factors on the broadening effect of diffraction maxima. In addition, the diffraction method is volumetric and therefore determines the size of crystallites averaged over the entire volume, in contrast to electron microscopy, which is a local visual method for estimating the size of particles (not crystallites) [25]. TEM results, to a certain extent, depend on the possibility of investigating only a relatively small number of particles under real conditions and on the quality of preliminary dispersion of nanopowders, which introduces a certain amount of uncertainty into the obtained results. Nevertheless, transmission electron microscopy is a direct and accurate method for determining the size and shape of nanoobject particles.

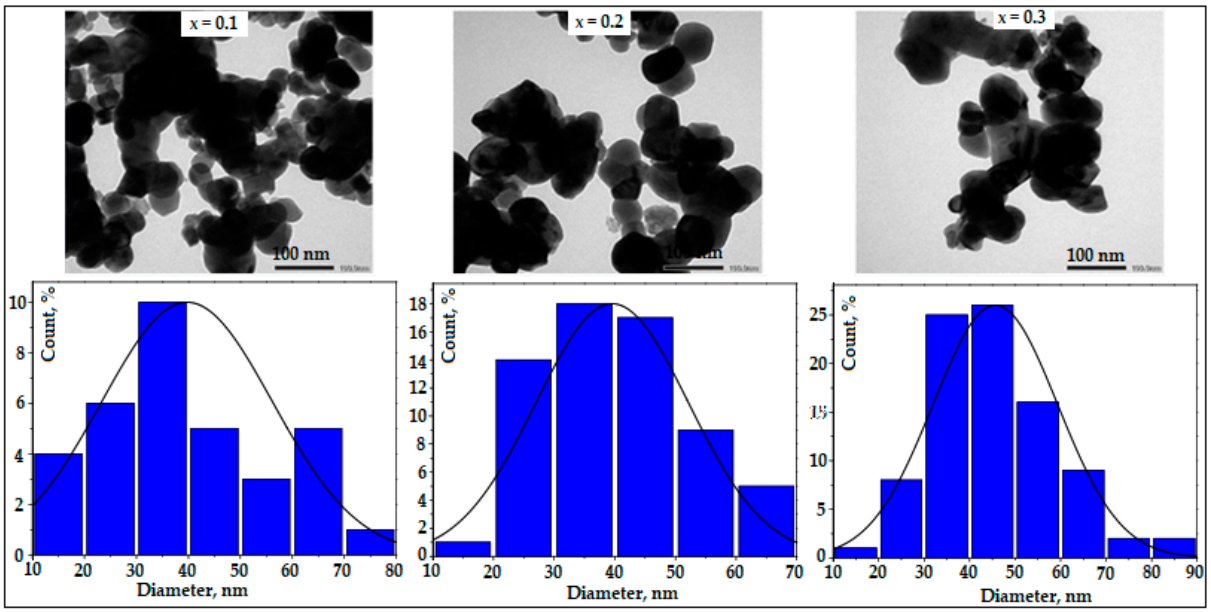

Figure 3. Transmission electron microscopy (TEM) images and particle size distribution of $NdFe_{1-x}Co_xO_3$ samples annealed at 750 °C.

3.2. Elemental Composition of $NdFe_{1-x}Co_xO_3$ Samples

According to the EDX results, the composition of the obtained $NdFe_{1-x}Co_xO_3$ samples included only Nd, Fe, Co, and O, and as the concentration of cobalt ions in the initial solutions increased, their content in the $NdFe_{1-x}Co_xO_3$ samples increased Table 2. From Table 2 it follows that the real content of each element in the synthesized samples is quite close to their nominal composition.

Table 2. EDX results of $NdFe_{1-x}Co_xO_3$ samples annealed at 750 °C for 60 min.

Nominal Composition of Samples	Elemental Composition (at. %)				Real Composition of Samples
	Nd	Fe	Co	O	
$NdFeO_3$	18.25 ± 1.57	20.45 ± 1.11	0.00	61.30 ± 2.17	$NdFe_{1.120}O_{3.359}$
$NdFe_{0.9}Co_{0.1}O_3$	18.95 ± 1.03	18.45 ± 1.07	1.43 ± 0.17	61.17 ± 2.36	$NdFe_{0.973}Co_{0.075}O_{3.228}$
$NdFe_{0.8}Co_{0.2}O_3$	19.01 ± 1.42	16.03 ± 0.89	2.13 ± 0.35	62.83 ± 3.21	$NdFe_{0.843}Co_{0.112}O_{3.305}$
$NdFe_{0.7}Co_{0.3}O_3$	19.27 ± 1.35	14.31 ± 0.73	5.41 ± 0.42	61.01 ± 3.08	$NdFe_{0.743}Co_{0.281}O_{3.166}$

3.3. Optical and Magnetic Properties of Nano-Structured $NdFe_{1-x}Co_xO_3$ (x = 0, 0.1, 0.2, and 0.3) Materials

The magnetic and optical characterizations of the $NdFe_{1-x}Co_xO_3$ (x = 0, 0.1, 0.2, and 0.3) nanomaterials (annealed at 750 °C for 60 min) were carried out at room temperature. The results prove that beside the structure, the substitution of Co in the $NdFeO_3$ crystal lattice also impressively change the magnetic and optical properties of the samples Table 3 and Figures 4 and 5.

Table 3. Optical and Magnetic characteristics of $NdFe_{1-x}Co_xO_3$ nanomaterials annealed at 750 °C for 60 min.

$NdFe_{1-x}Co_xO_3$	H_c, Oe	M_r, emu/g	M_s, emu/g	E_g, eV
$NdFeO_3$ [21]	136.76	0.68	0.80	2.06
$NdFe_{0.9}Co_{0.1}O_3$	258.22	0.13	0.93	1.74
$NdFe_{0.8}Co_{0.2}O_3$	395.79	0.15	0.97	1.53
$NdFe_{0.7}Co_{0.3}O_3$	416.06	0.18	0.98	1.46

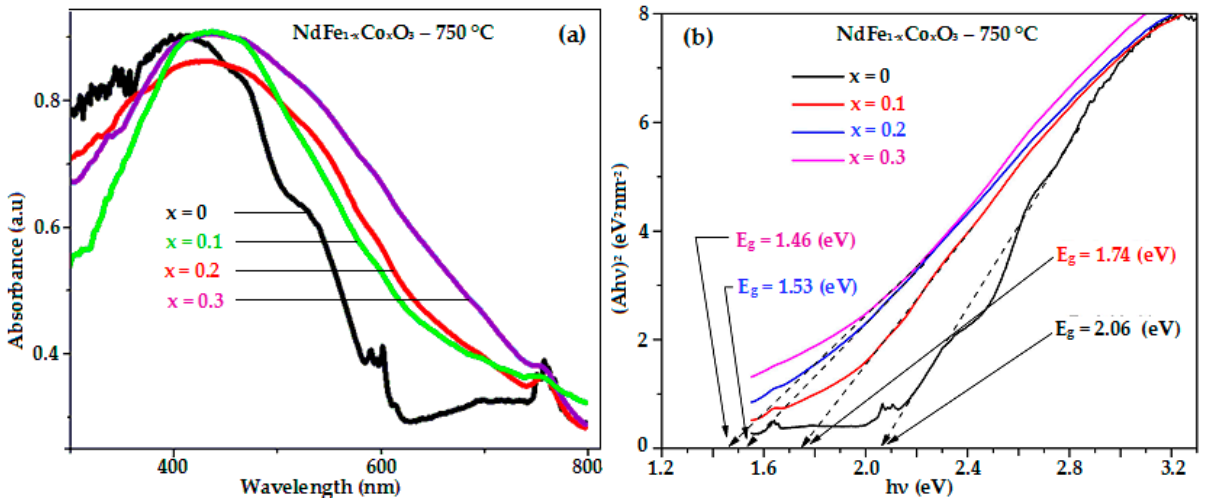

Figure 4. (**a**) Room-temperature optical absorbance spectra and (**b**) plot of $(Ahν)^2$ as a function of photon energy for $NdFe_{1-x}Co_xO_3$ materials annealed at 750 °C for 60 min.

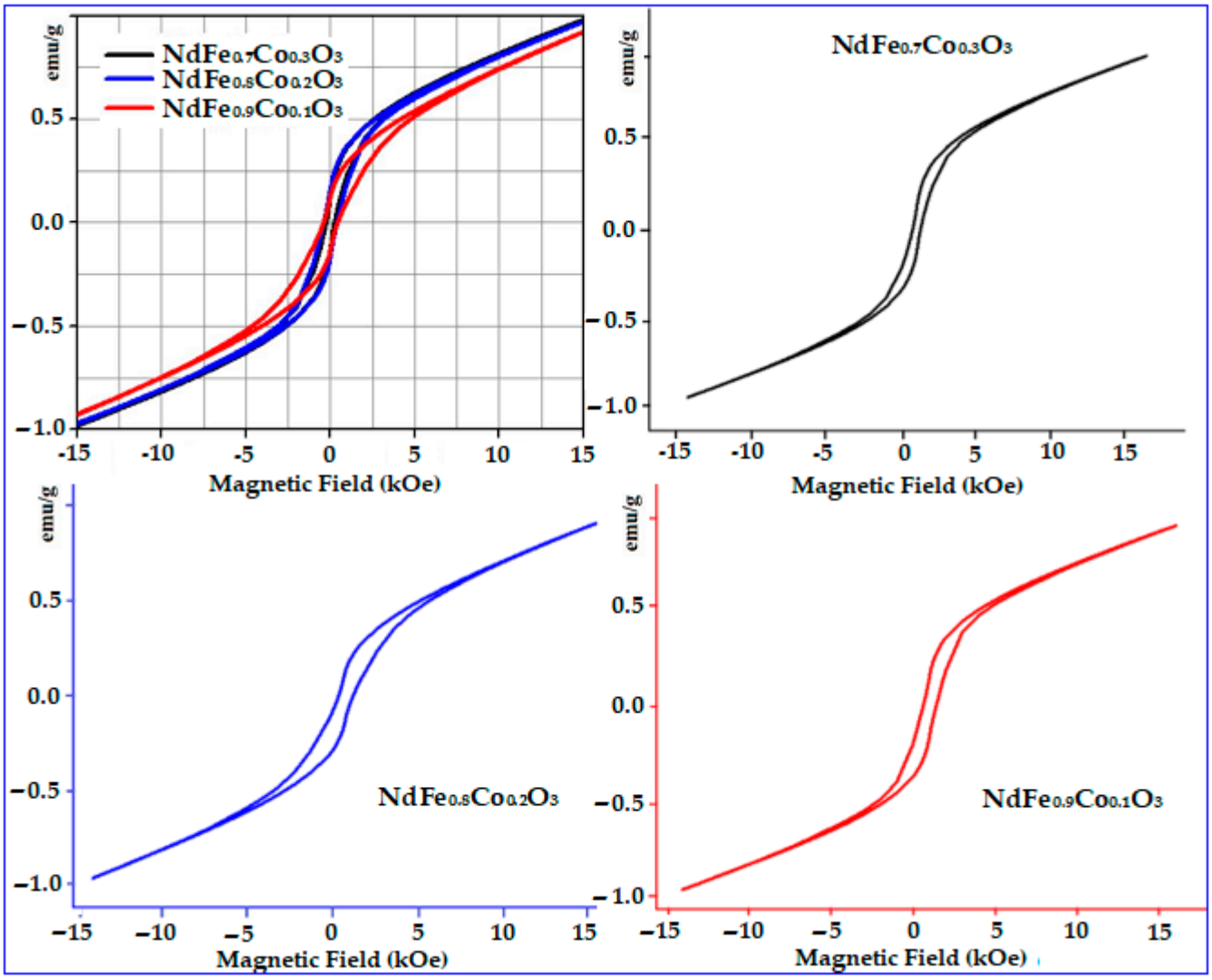

Figure 5. Field dependence of the magnetization of $NdFe_{1-x}Co_xO_3$ nanoparticles annealed at 750 °C for 60 min.

Indeed, when the concentration of Co ions in $NdFeO_3$ crystal lattice increased, all magnetic parameters, including H_c (258.22–416.04 Oe), M_s (0.93–0.98 emu/g), and M_r (0.13–0.18 emu/g) increased with the rise of Co concentration in the $NdFeO_3$ lattice. In addition, these values were significantly higher than those of the original $NdFeO_3$ material [21] (with the exception of M_r). It can be explained by the fact that the substitution of Co ions into the $NdFeO_3$ lattice can intensify the magneto-crystalline anisotropy. Besides, Co substitution also led to a change in Fe–O–Fe angles, as well as the oxidation of a small amount of Fe^{3+} ions to Fe^{4+} ions, to compensate for the charge caused by the appearance of Co^{2+} at the sites of Fe^{3+}. The similar phenomenon was also reported for $HoFe_{1-x}Ni_xO_3$ [26], $NdFe_{1-x}Ni_xO_3$ [27], $GdFe_{1-x}Ni_xO_3$ [28], $YFe_{1-x}Co_xO_3$ [18], and $LaFe_{1-x}Ni_xO_3$ series [19]. Remarkably, under the same synthesis conditions, the magnetic parameters, especially H_c, of the $NdFe_{1-x}Co_xO_3$ nano-crystalline perovskite oxides are higher than those of other perovskite oxides, such as $YFe_{1-x}Mn_xO_3$, $YFe_{1-x}Co_xO_3$, and $LaFe_{1-x}Ni_xO_3$ [17–19]. From those results, the magnetic properties of perovskite-type nanostructured materials can be easily tuned by varying the element and the degree of doping. This important feature of nanosized perovskites give them a wide variety of application in many different fields of magnetic materials.

The UV-Vis absorption spectra of the Co-doped $NdFeO_3$ nanoparticles showed strong absorption in the ultraviolet (~300–400 nm) and visible light regions (~400–600 nm) Figure 4a. As the concentration of Co ions increased, there was a red-shift in the UV-Vis absorption spectra (toward the visible light region). The optical energy gaps (E_g, eV) of the $NdFe_{1-x}Co_xO_3$ nanomaterials (x = 0, 0.1, 0.2, and 0.3) were calculated similarly to other publications [24,26] and are shown in Table 2 and Figure 4b. The estimated direct band gaps of all products are in the range of 2.06–1.46 eV and increase when Co content in $NdFeO_3$ lattice increases. Particularly, the Co-doped $NdFeO_3$ nanoparticles in this work exhibited much narrower band-gap compared to some other related orthoferrites synthesized by other methods. For instance, the direct band-gaps of $NdFe_{1-x}Co_xO_3$ (x = 0–0.4) and $HoFe_{1-x}Ni_xO_3$ (x = 0–0.5) nanoparticles were reported to be 3.35 ÷ 3.04 and 3.39 ÷ 3.28 eV, respectively [26,29], and the values for $LaFe_{1-x}Ti_xO_3$ (x = 0.2 ÷ 0.8) nanoparticles prepared by co-precipitation technique were 2.05–2.61 eV [2]. The small band gaps of $NdFe_{1-x}Co_xO_3$ can give an advantage for the application of this material series in photocatalysis, gas sensor, and electrode materials in solid oxide fuel cells [12,13,29–31].

4. Conclusions

The single-phase nanostructured $NdFe_{1-x}Co_xO_3$ (x = 0, 0.1, 0.2, and 0.3) perovskites have been synthesized by the simple co-precipitation method. The maximum level of substitution of iron with cobalt, which was $x < 0.4$ (XRD) was established. At x = 0.4, the homogeneity region was impaired and a phase mixture, consisting of Nd_2O_3 and Co_3O_4 was formed.

Obtained Co-doped $NdFeO_3$ nanoparticles, after annealing at 750 °C for 60 min, have their crystal size (D_{XRD} = 25 ± 3 ÷ 19 ± 3 nm, D_{TEM} = 47 ± 5 ÷ 42 ± 3 nm), unit cell volume (V = 238.56 ÷ 233.29 Å^3).

The study of the effect of the degree of substitution in $NdFe_{1-x}Co_xO_3$ crystals on their optical and magnetic characteristics showed that optical band-gap values (E_g = 2.06 ÷ 1.46 eV) decreased while the coercive force (H_c = 136.76 ÷ 416.06 Oe) and saturation magnetization (M_s = 0.80 ÷ 0.98 emu/g) increased with the increase of Co content. Co-doped $NdFeO_3$ nanoparticles have low optical energy gaps and high coercivity, which are beneficial not only for application in photocatalysis, but also for hard magnetic devices (permanent magnets or recorders).

Author Contributions: Conceptualization, T.A.N. and T.L.P.; methodology, T.A.N.; validation, I.Y.M., V.O.M. and V.X.B.; formal analysis, T.L.T.N. and H.V.N.; investigation, V.X.B. and H.V.N.; data curation, T.A.N. and T.L.P.; writing—original draft preparation, T.A.N., T.L.T.N. and I.Y.M.; writing—review and editing, V.O.M. and V.X.B. All authors have read and agreed to the published version of the manuscript.

Funding: This research received no external funding.

Data Availability Statement: Not Applicable.

Conflicts of Interest: The authors declare no conflict of interest.

References

1. Ahmad, I.; Akhtar, M.J.; Siddique, M.; Iqbal, M.; Hasan, M.M. Origin of anomalous octahedral distortions and collapse of magnetic ordering in $Nd_{1-x}Sr_xFeO_3$ ($0 \leq x \leq 0.5$). *Ceram. Int.* **2013**, *39*, 8901–8909. [CrossRef]
2. Sasikala, C.; Durairaj, N.; Baskaran, I.; Sathyaseelan, B.; Henini, M. Transition metal titanium (Ti) doped $LaFeO_3$ nanoparticles for enhanced optical structure and magnetic properties. *J. Alloys Compd.* **2017**, *712*, 870–877. [CrossRef]
3. Haron, W.; Thaweechai, T.; Wattanathana, W.; Laobuthee, A.; Manaspiya, H.; Veranitisagul, C.; Koonsaeng, N. Structure characteristics and dielectric properties of $La_{1-x}Co_xFeO_3$ and $LaFe_{1-x}Co_xO_3$ synthesized via metal organic complexes. *Energy Procedia* **2013**, *34*, 791–800. [CrossRef]
4. Xu, J.J.; Xu, D.; Wang, Z.L.; Wang, H.G.; Zhang, L.L.; Zhang, X.B. Synthesis of perovskite-based porous $La_{0.75}Sr_{0.25}MnO_3$ nanotubes as a highly efficient electrocatalyst for rechargeable lithium-oxygen batteries. *Angew. Chem. Int. Ed.* **2013**, *52*, 3887–3890. [CrossRef]
5. Tijare, S.N.; Bakardjieva, S.; Subrt, J.; Joshi, M.V.; Rayalu, S.S.; Hishita, S.; Labhsetwar, N. Synthesis and visible light photocatalytic activity of nanocrystalline $PrFeO_3$ perovskite for hydrogen generation in ethanol-water system. *J. Chem. Sci.* **2014**, *125*, 517–525. [CrossRef]
6. Megarajan, S.K.; Rayalu, S.; Nishibori, M.; Labhsetwar, N. Improved catalytic activity of $PrFeO_3$ (M = Co and Fe) perovskites: Synthesis of thermally stable nanoparticles by a novel hydrothermal method. *N. J. Chem.* **2015**, *39*, 2345–2348. [CrossRef]
7. Shin, N.; Isao, A.; Yasuhiko, I.; Takeo, H. Preparation of $Y(Mn_{1-x}Fe_x)O_3$ and electrical properties of the sintered bodies. *Open J. Inorg. Chem.* **2015**, *5*, 54514589.
8. Fang, F.; Zhao, P.; Feng, N.; Wan, H.; Guan, G. Surface engineering on popous perovskite-type $La_{0.6}Sr_{0.4}CoO_{3-\delta}$ nanotubes for an enhanced performance in diesel soot elimination. *J. Hazadous Mater.* **2020**, *399*, 123014. [CrossRef]
9. Mir, F.A.; Sharma, S.K.; Kumar, R. Magnetizations and magneto-transport properties of Ni-doped $PrFeO_3$ thin films. *Chin. Phys. B* **2014**, *23*, 048101. [CrossRef]
10. Yuan, S.J.; Ren, W.; Hong, F.; Wang, Y.B.; Zhang, J.C.; Bellaiche, L.; Cao, S.X.; Cao, G. Spin switching and magnetization reversal in single-crystal $NdFeO_3$. *Phys. Rev. B* **2013**, *87*, 184405. [CrossRef]
11. Pekinchak, O.; Vasylechko, L.; Lutsyuk, I.; Vakhula, Y.; Prots, Y.; Cabrera, W.C. Sol-gel prepared nanoparticles of mixed praseodymium cobaltites ferrites. *Nanoscale Res. Lett.* **2016**, *11*, 75. [CrossRef] [PubMed]
12. Zhang, R.; Hu, J.; Han, Z.; Zhao, M.; Wu, Z.; Zhang, Y.; Qin, H. Electrical and CO-sensing properties of $NdFe_{1-x}Co_xO_3$ perovskite system. *J. Rare Earths* **2010**, *28*, 591–595. [CrossRef]
13. Feng, C.; Ruan, S.; Li, J.; Zou, B.; Luo, J.; Chen, W.; Dong, W.; Wu, F. Ethanol sensing properties of $LaCo_xFe_{1-x}O_3$ nanoparticles: Effects of calcination temperature, Co-doping, and carbon nanotube-treatment. *Sens. Actuators B Chem.* **2011**, *155*, 232–238. [CrossRef]
14. Zhou, Z.; Guo, L.; Yang, H.; Liu, Q.; Ye, F. Hydrothermal synthesis and magnetic properties of multiferroic rare-earth orthoferrites. *J. Alloys Compd.* **2014**, *583*, 21–31. [CrossRef]
15. Nguyen, T.A.; Mittova, I.Y.; Almjasheva, O.V.; Kirillova, S.A.; Gusarov, V.V. Influence of the preparation conditions on the size and morphology of nanocrystalline lanthanum orthoferrite. *Glass Phys. Chem.* **2008**, *34*, 756–761.
16. Nguyen, A.T.; Almjasheva, O.V.; Mittova, I.Y.; Stognei, O.V.; Soldatenko, S.A. Synthesis and magnetic properties of $YFeO_3$ nanocrystals. *Inorg. Mater.* **2009**, *45*, 1304–1308.
17. Nguyen, A.T.; Pham, V.N.; Nguyen, T.T.L.; Mittova, V.O.; Vo, Q.M.; Berezhnaya, M.V.; Mittova, I.Y.; Do, T.H.; Chau, H.D. Crystal structure and magnetic properties of perovskite $YFe_{1-x}Mn_xO_3$ nanopowders synthesized by co-precipitation method. *Solid State Sci.* **2019**, *96*, 105922. [CrossRef]
18. Nguyen, T.A.; Chau, D.H.; Nguyen, L.T.T.; Mittova, V.O.; Do, H.T.; Mittova, I.Y. Structural and magnetic properties of $YFe_{1-x}Co_xO_3$ ($0.1 \leq x \leq 0.5$) perovskite nanomaterials synthesized by co-precipitation method. *Nanosyst. Phys. Chem. Math.* **2018**, *9*, 424–429. [CrossRef]
19. Nguyen, T.A.; Pham, V.N.T.; Le, H.T.; Chau, D.H.; Mittova, V.O.; Nguyen, L.T.T.; Dinh, D.A.; Hao, T.V.N.; Mittova, I.Y. Crystal structure and magnetic properties of $LaFe_{1-x}Ni_xO_3$ nanomaterials prepared via a simple co-precipitation method. *Ceram. Int.* **2019**, *45*, 21768–21772. [CrossRef]
20. Nguyen, T.A.; Pham, V.; Chau, D.H.; Mittova, V.O.; Mittova, I.Y.; Kopeychenko, E.L.; Nguyen, L.T.T.; Bui, V.X.; Nguyen, A.T.P. Effect of Ni substitution on phase transition, crystal structure and magnetic properties of nanostructured $YFeO_3$ perovskite. *J. Mol. Struct.* **2020**, *1215*, 128293. [CrossRef]
21. Nguyen, T.A.; Pham, V.; Pham, T.L.; Nguyen, L.T.T.; Mittova, I.Y.; Mittova, V.O.; Vo, L.N.; Nguyen, B.T.T.; Bui, V.X.; Viryutina, E.L. Simple synthesis of $NdFeO_3$ by the so-precipitation method based on a study of thermal behaviors of Fe (III) and Nd (III) hydroxides. *Crystals* **2020**, *10*, 219. [CrossRef]
22. Housecroft, C.E.; Sharpe, A.G. *Inorganic Chemistry*, 2nd ed.; Pearson, Prentice Hall: Upper Saddle River, NJ, USA, 2005; 950p.

23. Yousefi, M.; Zeid, S.S.; Motlagh, M.K. Synthesis and characterization of nano-structured perovskite type neodymium orthoferrite $NdFeO_3$. *Curr. Chem. Lett.* **2017**, *6*, 23–30. [CrossRef]
24. Ghobadi, N. Band gap determination using absorption spectrum fitting procedure. *Int. Nano Lett.* **2013**, *3*, 2. [CrossRef]
25. Knurova, M.V.; Mittova, I.Y.; Perov, N.S.; Al'myasheva, O.V.; Nguyen, T.A.; Mittova, V.O.; Bessalova, V.V.; Viryutina, E.L. Effect of the degree of doping on the size and magnetic properties of nanocrystals $La_{1-x}Zn_xFeO_3$ synthesized by the sol-gel method. *Russ. J. Inorg. Chem.* **2017**, *62*, 281–287. [CrossRef]
26. Habib, Z.; Majid, K.; Ikram, M.; Sultan, K. Influence of Ni substitution at B-site for Fe^{3+} ions on morphological, optical, and magnetic properties of $HoFeO_3$ ceramics. *Appl. Phys. A Mater. Sci. Process.* **2016**, *12*, 550. [CrossRef]
27. Mir, S.A.; Ikram, M.; Asokan, K. Effect of Ni doping on optical, electrical and magnetic properties of Nd orthoferrite. *J. Phys. Conf. Ser.* **2014**, *534*, 012017. [CrossRef]
28. Bashir, A.; Ikram, M.; Kumar, R.; Lisboa-Filho, P.N. Structural, electronic structure and magnetic studies of $GdFe_{1-x}Ni_xO_3$ ($x \leq 0.5$). *J. Alloys Compd.* **2012**, *521*, 183–188. [CrossRef]
29. Somvanshi, A.; Husain, S.; Khan, W. Investigation of structure and physical properties of cobalt doped nano-crystalline neodymium orthoferrite. *J. Alloys Compd.* **2019**, *778*, 439. [CrossRef]
30. Nguyen, T.A.; Nguyen, L.T.T.; Bui, V.X.; Nguyen, D.H.; Lieu, H.D.; Le, L.M.; Pham, V. Optical and magnetic properties of $HoFeO_3$ nanocrystals prepared by a simple co-precipitation method using ethanol. *J. Alloys Compd.* **2020**, *834*, 155098. [CrossRef]
31. Phokha, S.; Pinitsoontorn, S.; Maensiri, S.; Rujirawat, S. Structure, optical and magnetic properties of $LaFeO_3$ nanoparticles prepared by polymerized complex method. *J. Sol Gel Sci. Technol.* **2014**, *71*, 333–341. [CrossRef]